*The Canadian Mineralogist*
Vol. 48, pp. 29-40 (2010)
DOI: 10.3749/canmin.48.1.29

# DEVITOITE, A NEW HETEROPHYLLOSILICATE MINERAL WITH ASTROPHYLLITE-LIKE LAYERS FROM EASTERN FRESNO COUNTY, CALIFORNIA

ANTHONY R. KAMPF[§]

*Mineral Sciences Department, Natural History Museum of Los Angeles County, 900 Exposition Boulevard, Los Angeles, California 90007, U.S.A.*

GEORGE R. ROSSMAN

*Division of Geological and Planetary Sciences, California Institute of Technology, Pasadena, California 91125–2500, U.S.A.*

IAN M. STEELE AND JOSEPH J. PLUTH

*Department of the Geophysical Sciences, The University of Chicago, 5734 S. Ellis Avenue, Chicago, Illinois 60637, U.S.A.*

GAIL E. DUNNING

*773 Durshire Way, Sunnyvale, California 94087, U.S.A.*

ROBERT E. WALSTROM

*P. O. Box 1978, Silver City, New Mexico 88062, U.S.A.*

## ABSTRACT

Devitoite, $[Ba_6(PO_4)_2(CO_3)]$ $[Fe^{2+}{}_7Fe^{3+}{}_2(Si_4O_{12})_2O_2(OH)_4]$, is a new mineral species from the Esquire #8 claim along Big Creek in eastern Fresno County, California, U.S.A. It is also found at the nearby Esquire #7 claim and at Trumbull Peak in Mariposa County. The mineral is named for Alfred (Fred) DeVito (1937–2004). Devitoite crystallized very late in a sequence of minerals resulting from fluids interacting with a quartz–sanbornite vein along its margin with the country rock. The mineral occurs in subparallel intergrowths of very thin brown blades, flattened on {001} and elongate and striated parallel to [100]. The mineral has a cream to pale brown streak, a silky luster, a Mohs hardness of approximately 4, and two cleavages: {001} perfect and {010} good. The calculated density is 4.044 g/cm$^3$. It is optically biaxial (+), $\alpha$ 1.730(3), $\beta$ 1.735(6), $\gamma$ 1.755(3); $2V_{calc}$ = 53.6°; orientation: $X \approx b$, $Y \approx c$, $Z \approx a$; pleochroism: brown, $Y >>> X > Z$. Normalized electron-microprobe analyses provided: BaO 38.83, CaO 0.50, MgO 0.75, FeO 22.02, $Fe_2O_3$ 6.08, $Al_2O_3$ 1.50, $SiO_2$ 20.97, $TiO_2$ 0.80, $P_2O_5$ 4.84, $H_2O$ 1.67, $CO_2$ 2.04, total 100.00 wt%, with FeO and $Fe_2O_3$ assignments and $H_2O$ and $CO_2$ based on the structure. The empirical formula is $[(Ba_{5.45}Ca_{0.19})_{\Sigma 5.64}(PO_4)_{1.47}O_{0.30}(CO_3)]$ $[(Fe^{2+}{}_{6.60}Mg_{0.40})_{\Sigma 7}(Fe^{3+}{}_{1.64}Ti^{4+}{}_{0.22}Al^{3+}{}_{0.14})_{\Sigma 2}(Si_{7.51}Al_{0.49})_{\Sigma 8}O_{26}(OH)_4]$. Devitoite is triclinic, $P\bar{1}$, $a$ 5.3437(7), $b$ 11.6726(15), $c$ 14.680(2) Å, $\alpha$ 91.337(4), $\beta$ 96.757(4), $\gamma$ 103.233(4)°, $V$ 884.0(2) Å$^3$ and $Z = 1$. The crystal-structure determination ($R_1 = 9.56\%$ for 1370 $F_o > 4\sigma F$) shows the mineral to be a heterophyllosilicate with astrophyllite-type *HOH* layers in which five-coordinated $Fe^{3+}$ takes the place of $Ti^{4+}$. The interlayer region contains Ba atoms, $PO_4$ groups and $CO_3$ groups. The configuration of the Ba and $PO_4$ in the interlayer region is similar to that found in the structure of yoshimuraite.

*Keywords*: devitoite, new mineral species, crystal structure, heterophyllosilicate, astrophyllite layers, Big Creek – Rush Creek sanbornite deposits, California.

## SOMMAIRE

Nous décrivons la devitoïte, $[Ba_6(PO_4)_2(CO_3)]$ $[Fe^{2+}{}_7Fe^{3+}{}_2(Si_4O_{12})_2O_2(OH)_4]$, nouvelle espèce minérale provenant du claim Esquire #8 le long de Big Creek, dans le secteur oriental du comté de Fresno, en Californie. On la trouve aussi sur le claim Esquire #7 à Trumbull Peak, comté de Mariposa. Le nom choisi est à la mémoire de Alfred (Fred) DeVito (1937–2004). La devitoïte aurait cristallisé très tardivement dans une séquence de minéraux résultant de l'interaction entre une phase fluide dans une veine à quartz–sanbornite et les roches encaissantes. Le minéral se présente en intercroissances subparallèles de lamelles brunes très

§ *E-mail address*: akampf@nhm.org

minces, aplaties sur {001} et allongées selon [100]. Il a une rayure crème à brun pâle, un éclat soyeux, une dureté de Mohs d'environ 4, et deux clivages, {001} parfait et {010} bon. La densité calculée est 4.044 g/cm$^3$. Il s'agit d'un minéral optiquement biaxe (+), $\alpha$ 1.730(3), $\beta$ 1.735(6), $\gamma$ 1.755(3); $2V_{calc}$ = 53.6°; orientation: $X \approx b$, $Y \approx c$, $Z \approx a$; pleochroïsme: brun $Y >>> X > Z$. Les résultats normalisés d'analyses à la microsonde électronique ont donné: BaO 38.83, CaO 0.50, MgO 0.75, FeO 22.02, $Fe_2O_3$ 6.08, $Al_2O_3$ 1.50, $SiO_2$ 20.97, $TiO_2$ 0.80, $P_2O_5$ 4.84, $H_2O$ 1.67, $CO_2$ 2.04, pour un total de 100.00% (poids), avec FeO et $Fe_2O_3$ attribués, et $H_2O$ et $CO_2$ quantifiés selon la structure. La formule empirique serait $[(Ba_{5.45}Ca_{0.19})_{\Sigma 5.64}(PO_4)_{1.47}O_{0.30}(CO_3)]$ $[(Fe^{2+}_{6.60}Mg_{0.40})_{\Sigma 7}$ $(Fe^{3+}_{1.64}Ti^{4+}_{0.22}Al^{3+}_{0.14})_{\Sigma 2}$ $(Si_{7.51}Al_{0.49})_{\Sigma 8}O_{26}(OH)_4]$. La devitoïte est triclinique, $P\bar{1}$, $a$ 5.3437(7), $b$ 11.6726(15), $c$ 14.680(2) Å, $\alpha$ 91.337(4), $\beta$ 96.757(4), $\gamma$ 103.233(4)°, $V$ 884.0(2) Å$^3$ et $Z$ = 1. D'après sa structure cristalline ($R_1$ = 9.56% pour 1370 $F_o > 4\sigma F$), le minéral serait un hétérophyllosilicate avec les couches *HOH* typiques de l'astrophyllite dans lesquelles le $Fe^{3+}$ en coordinence cinq joue le rôle du $Ti^{4+}$. La région entre les feuillets contient des atomes de Ba, des groupes $PO_4$, et des groupes $CO_3$. La configuration de Ba et de $PO_4$ dans la région intercouche ressemble à celle de la yoshimuraïte.

(Traduit par la Rédaction)

*Mots-clés*: devitoïte, nouvelle espèce minérale, structure cristalline, hétérophyllosilicate, couches typiques de l'astrophyllite, gisement de sanbornite Big Creek – Rush Creek, Californie.

## Introduction

The sanbornite deposits located along Big Creek and Rush Creek (Walstrom & Leising 2005) in Fresno County and at Trumbull Peak (Dunning & Cooper 1999) in Mariposa County, California, U.S.A. have yielded a wealth of exotic minerals, including 12 new species: from Trumbull Peak, sanbornite (Rogers 1932) and fencooperite (Roberts *et al.* 2001), and from Big Creek and Rush Creek, fresnoite, krauskopfite, macdonaldite, muirite, traskite, verplanckite, and walstromite (Alfors *et al.* 1965), alforsite (Newberry *et al.* 1981), bigcreekite (Basciano *et al.* 2001a) and kampfite (Basciano *et al.* 2001b). Several additional new species from Big Creek and Rush Creek remain under study, including the $Fe^{2+}$ and Al analogues of cerchiaraite (minerals 10a and 10b), the $Fe^{2+}$ analogue of ericssonite (mineral 39), and a hydrated silica phase (mineral 21). The new species reported herein was discovered by one of the authors (REW) in 1982 at the Esquire #8 claim on Big Creek, and was referred to in previous reports (*e.g.*, Walstrom & Leising 2005) as mineral 27.

The species is named for Alfred (Fred) DeVito (1937–2004), for many years one of California's leading micromounters and field collectors. Fred was best known for his expertise on the minerals of Crestmore Quarry, Riverside County, California, and for his prolific collecting of zeolites in the Santa Monica Mountains of Southern California. He contributed generously to the mineralogical community, publishing articles, presenting lectures, serving as president of several organizations, providing specimens for scientific research and as donations to various museums. In his later years, Fred lived in Oakhurst, California, a short distance from the sanbornite deposits along Big Creek and Rush Creek, and had begun to actively involve himself in the study of their mineralogy.

The new mineral and name have been approved by the Commission on New Minerals, Nomenclature and Classification of the International Mineralogical Association (IMA 2009–010). The four cotype specimens used in the description of the mineral are housed in the mineral collection of the Natural History Museum of Los Angeles County (catalogue numbers 61591, 61592, 61593 and 61594).

## Occurrence

The mineral occurs at the Esquire #8 claim along Big Creek in SE¼ SW¼, Section 22, T11S, R25E, Mount Diablo Meridian, eastern Fresno County, California, USA (36°56'42"N, 119°14'12"W). It crystallized very late in a sequence of minerals resulting from fluids interacting with a quartz–sanbornite vein along its margin with the country rock. It occurs along cleavage planes of altered gillespite and is closely associated with titantaramellite, celsian, anandite, quartz and the $Fe^{2+}$ analogue of ericssonite (currently under study). From textural relationships, the mineral and the $Fe^{2+}$ analogue of ericssonite appear to be products of the alteration of gillespite. The parallel bedding also hosts bazirite, edingtonite, fresnoite, macdonaldite, pellyite, sanbornite, Ba-rich tobermorite, walstromite and witherite. The paragenetic position of the new mineral places it later than celsian, gillespite, sanbornite, titantaramellite and walstromite. A description of the mineralogy of the sanbornite deposits along Big Creek and Rush Creek in eastern Fresno County, California is provided by Walstrom & Leising (2005).

The mineral has also been identified as a very rare phase at two other localities. At the Esquire #7 claim (along Big Creek approximately 1 km south of the Esquire #8 claim), it occurs as an alteration product of gillespite along parting planes associated with the $Fe^{2+}$ analogue of ericssonite and minor anandite. At Trumbull Peak, Mariposa County, California, it occurs in a gillespite–sanbornite rock associated with titantaramellite and fencooperite (Dunning & Cooper 1999).

## Physical and Optical Properties

Devitoite occurs as thin brown blades, flattened on {001}, elongate and striated parallel to [100], without obvious terminations (Fig. 1). Individual crystals can reach 5 mm in length and 0.3 mm in width, but are generally much smaller, and their thickness rarely exceeds 1 μm. Crystals invariably occur in subparallel intergrowths. No twinning was observed.

The streak is cream to pale brown. Crystals are transparent to translucent with a silky luster. The Mohs hardness is estimated to be approximately 4. The tenacity is flexible, the fracture is irregular, and there is one perfect cleavage on {001} and one good cleavage on {010}. We encountered difficulty in using the sink–float method with Clerici solution because the density is so close to that of a saturated Clerici solution (4.2 g/cm$^3$). The density calculated from the empirical formula is 4.044 g/cm$^3$. Crystals decompose very slowly in dilute HCl, turning white and opaque.

The mineral is optically biaxial (+), with the following optical constants measured in white light: α 1.730(3), β 1.735(6) and γ 1.755(3). The $2V$ and dispersion could not be determined because of the unfavorable shape of the crystals. The unfavorable orientation also made the determination of β more difficult. The calculated $2V$ is 53.6°. Pleochroism is brown, $Y >>> X > Z$. The optical orientation is $X \approx b$, $Y \approx c$, $Z \approx a$. Extinction is approximately parallel to the length of the blades in all orientations.

## Spectroscopy

Infrared absorption spectra were obtained with a Nicolet Magna 860 FTIR and a Nicolet Continuμm infrared microscope with a $LN_2$-cooled MCT–A detector. The sample used for the infrared spectra is a relatively flat, single 49 × 123 × ~5 μm thick blade mounted on a thin $BaF_2$ slab for support. The uncertainty in the thickness is due to the unevenness in the broad faces of the blade. Two sets of spectra were obtained. The first was with a $CaF_2$ beamsplitter for high-sensitivity studies of the OH region, and the second used a KBr beamsplitter to cover both the OH and carbonate regions. In the first set of spectra (Fig. 2), a prominent OH band appears at 3559 cm$^{-1}$ that confirms the presence of OH, indicated by the structure determination. The OH bands show modest polarization with the greater intensity in the E ∥ $a$ direction. The broad features between 1550 and 1750 cm$^{-1}$ are in a region where absorption due to molecular $H_2O$ may occur; however, as explained below, the OH indicated by the structure determination is more than sufficient to account for the size of the OH band at 3559 cm$^{-1}$. We suggest, therefore, that the absorption in the vicinity of 1600 cm$^{-1}$ more likely arises from other causes. In the second set (Fig. 3), both the OH and carbonate bands are seen. The intense carbonate band at about 1410 cm$^{-1}$ is strongly polarized, confirming that the carbonate group is present and oriented dominantly in the $a$–$c$ plane, also consistent with the structure determination. Weak features from contamination from organic materials appear in the 2900 cm$^{-1}$ region.

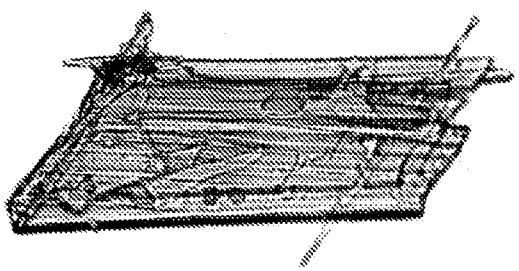

FIG. 1. Fragment of a devitoite crystal (49 × 123 × ~5 μm) used in IR study (Figs. 2, 3).

To independently confirm the $H_2O$ content determined from the structure determination discussed below, a rough estimate of the amount of OH in the crystal can be obtained from the infrared spectra if a pair of assumptions is accepted. The infrared spectra have been obtained in only two of the three orientations of the crystal. The first assumption is that the spectra in the missing orientation is the average of the other two directions; a total integrated area of the OH bands in the 3550 cm$^{-1}$ region is 43,700 cm$^{-2}$. The relationship between the absolute amount of OH and the intensity of the infrared spectrum has been calibrated for only a small number of minerals; in particular, the relationship has never been calibrated for devitoite. Using a second assumption that this relationship is similar to the calibration for hydrogrossular (Rossman & Aines 1991), a concentration of 1.2% (as $H_2O$) is estimated from the infrared spectra. Similar assumptions taken from calibrations in other mineral systems also put the $H_2O$ content in the 1 to 2% range, consistent with the structural results indicating that there is 1.67 wt.% $H_2O$ in devitoite.

Raman spectroscopic micro-analysis was carried out using a Renishaw M1000 micro-Raman spectrometer system. Spectra were obtained with a 514.5 nm argon ion laser and with a 100× objective, producing a spot about 0.9 micrometers in diameter with about 2.5 mW power. (Sample decomposition was noted almost immediately with 5 mW power.) Peak positions were calibrated against a silicon standard. A dual-wedge polarization scrambler was used in the laser beam for all spectra to minimize the effects of polarization. The Raman spectra were quite weak. They were obtained on multiple crystals to ensure that artifacts or contaminants were not part of the reported data. Because of the low intensity of the Raman signal, multiple slow scans were accumulated. The Raman data were baseline-corrected

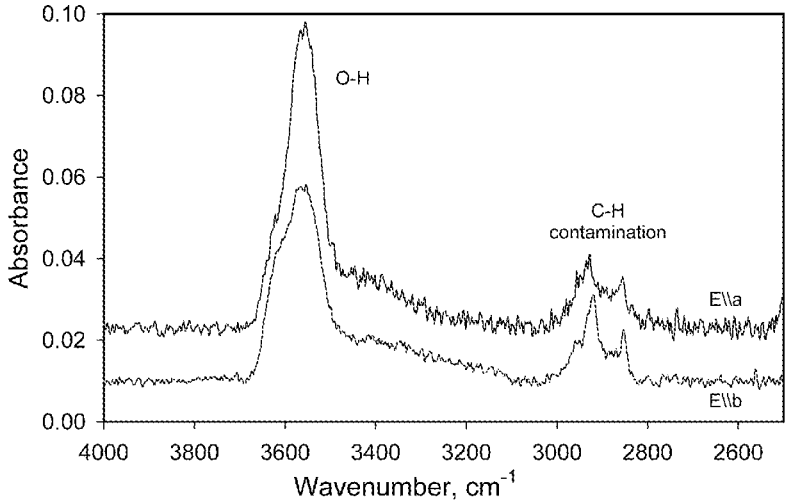


FIG. 2. Devitoite: infrared absorption spectra in two polarizations. The E || *a* curve is offset vertically by 0.01 for clarity.

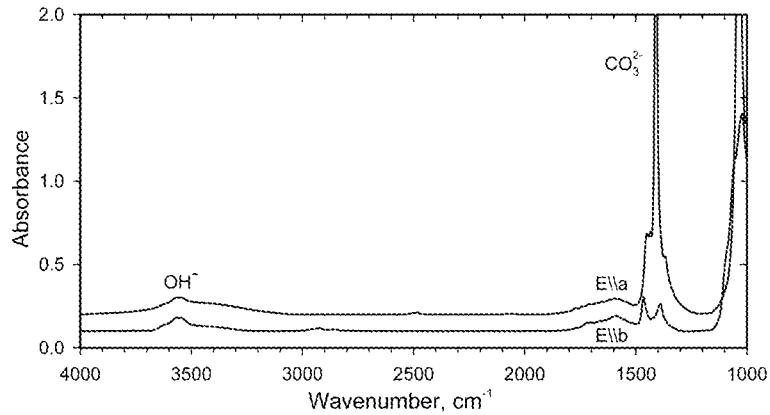


FIG. 3. Devitoite: infrared absorption spectra in two polarizations covering both the OH and carbonate regions. Curves are offset slightly vertically for clarity.

for a set of broad, moderately intense, overlapping fluorescence-induced features centered near 1600, 2100, 2500, and 2900 $cm^{-1}$ using a subjective, manual baseline-correction procedure within the instrument's software.

The Raman bands (Fig. 4) are found at 1072 $cm^{-1}$ (medium), 1053 $cm^{-1}$ (medium), 914 $cm^{-1}$ (strongest), 660 $cm^{-1}$ (medium), with a shoulder near 700 $cm^{-1}$, 463 $cm^{-1}$ (weakest, the least reliable of the bands), and 243 $cm^{-1}$ (weak). The OH bands near 3550 $cm^{-1}$ and the carbonate bands near 1410 $cm^{-1}$ were not observed in the Raman spectra. There is considerable overlap in the positions of the Raman bands of phosphates, carbonates and silicates. Both phosphates and carbonates have bands in the 250 $cm^{-1}$ region. Phosphates are more likely to have bands in the 420 and 650 $cm^{-1}$ region, and carbonates are more likely to be in the 700 $cm^{-1}$ range. In the 900 to 1100 $cm^{-1}$ region, phosphate bands are expected to be generally at lower wavenumbers than those for carbonates. The strongest bands in the spectrum of the $Fe^{2+}$ layer silicates, annite and astrophyllite, are also in 700 $cm^{-1}$ region (Downs 2006). Because of the overlap, specific assignments of the bands have not been made.

Digital versions of the infrared and Raman spectra are available from the Depository of Unpublished Data on the MAC website [document Devitoite CM48_29].

## Chemical Composition

Quantitative chemical analyses were performed with an electron microprobe (WDS mode, 15 kV, 25 nA, beam diameter 5 μm). The structure refinement indicates the presence of $CO_3$ and OH, and this is corroborated by the IR spectrum. The small amount of material available did not allow the direct determination of $H_2O$ or $CO_2$, so these were calculated from the structure.

Even considering the $H_2O$ and $CO_2$ content discussed above, the EMP analyses gave significantly low totals, by about 6.5% relative to the structural formula; however, cation ratios derived from the analyses fit the structural formula well. During the analyses, count rates for the major elements were carefully monitored as a function of time and showed no decreases that might be indicative of element burn-off or sample degradation. The possible presence of other elements (such as S, which might substitute for P) was also investigated in detail, but none were found. We did observe the reflectivity of the polished surfaces of the mounted crystals to decrease over time in the EMP vacuum, a possible indication of volatile loss; however, for volatile loss alone to be a significant cause of the low totals would imply a much greater volatile ($H_2O$ and $CO_2$) content than is indicated by the structure determination. We favor an explanation for the low EMP totals that couples volatile loss from the interlayer region with a resultant increase in the porosity of the sample.

The EMP analyses provided, on average, in wt%, BaO 36.30, CaO 0.47, MgO 0.70, FeO 25.70, $Al_2O_3$ 1.40, $SiO_2$ 19.60, $TiO_2$ 0.75, $P_2O_5$ 4.52. The cation proportions from the EMP analyses were used to derive an empirical formula such that the layer portion contains 17 cations (Fe + Mg + Al + Si + Ti = 17), 30 O atoms and 4 H atoms, with $Fe^{2+}$ and $Fe^{3+}$ allocated in accord with the structure, and the interlayer portion contains 1 C atom and sufficient O atoms to balance the overall charge. This yields $[(Ba_{5.45}Ca_{0.19})_{\Sigma 5.64}(PO_4)_{1.47}O_{0.30}(CO_3)]$ $[(Fe^{2+}_{6.60}Mg_{0.40})_{\Sigma 7}$ $(Fe^{3+}_{1.64}Ti^{4+}_{0.22}Al^{3+}_{0.14})_{\Sigma 2}$ $(Si_{7.51}Al_{0.49})_{\Sigma 8}O_{26}(OH)_4]$, which corresponds to BaO 38.83, CaO 0.50, MgO 0.75, FeO 22.02, $Fe_2O_3$ 6.08, $Al_2O_3$ 1.50, $SiO_2$ 20.97, $TiO_2$ 0.80, $P_2O_5$ 4.84, $H_2O$ 1.67, $CO_2$ 2.04, total 100.00 wt%. This reflects the normalized EMP analyses, with $H_2O$ and $CO_2$ derived from the structure as discussed above. The simplified formula is $[Ba_6(PO_4)_2(CO_3)]$ $[Fe^{2+}_7Fe^{3+}_2(Si_4O_{12})_2O_2(OH)_4]$, which requires BaO 40.26, FeO 22.01, $Fe_2O_3$ 6.99, $SiO_2$ 21.03, $P_2O_5$ 6.21, $H_2O$ 1.58, $CO_2$ 1.93, total 100.00 wt%.

The Gladstone–Dale compatibility index $1 - (K_P/K_C)$, as defined by Mandarino (1981), provides a measure of the consistency among the average index of refraction, calculated density and chemical composition. For devitoite, the compatibility index is –0.026, indicating excellent agreement among these data.

## X-Ray Crystallography and Structure Determination

Powder X-ray diffraction data were obtained on a Rigaku R-Axis Spider curved imaging plate microdiffractometer utilizing monochromatized Mo$K\alpha$ radiation. The powder data are presented in Table 1. The unit-cell parameters refined from the powder data are $a$ 5.3533(3), $b$ 11.6953(5), $c$ 14.6816(8) Å, α 91.197(5), β 96.844(5), γ 103.277(5)°, $V$ 887.14(6) Å$^3$.

A single crystal with the dimensions 80 × 40 × 3 μm was used for the first collection of structure data at the facilities of ChemMatCARS, Sector 15, Advanced

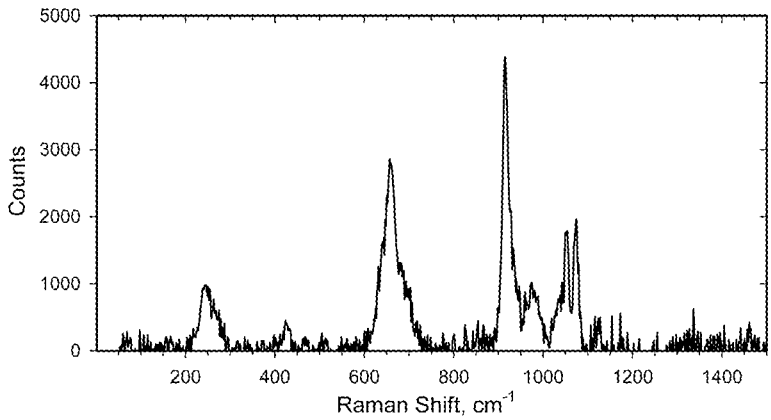


FIG. 4. Baseline-corrected Raman spectrum of devitoite.

Photon Source at Argonne National Laboratory, USA. Data were collected at 293 K using radiation of wavelength 0.41328 Å with a Bruker 6000 SMARTCCD detector mounted on a Huber four-circle diffractometer. The data were integrated and corrected for Lorentz, polarization, and background effects and systematic errors, such as beam decay and absorption, using SAINTPLUS and SADABS (Bruker 2005). Efforts to solve the structure from these data using direct methods in SHELXS–97 (Sheldrick 2008) were only partially successful ($R_1$ = 23%). The general motif of the structure was revealed, but several O atoms could not be unambiguously located, and the C atom was not revealed. The incompleteness of the solution is attributed to the poor quality of the crystal used.

Subsequently, a better crystal measuring 130 × 23 × 1 μm was used for data collection on the same Rigaku R-Axis Spider instrument used to obtain the powder-diffraction data, also utilizing monochromatized Mo$K\alpha$ radiation. The Rigaku CRYSTALCLEAR software package was used for processing of the structure data. The SHELXL97 software (Sheldrick 2008) was used for the solution and refinement of the structure. The E-statistics did not unambiguously indicate the centricity. The centrosymmetric space-group $P\bar{1}$ was ultimately chosen because efforts to refine the structure in $P1$ led to unreasonable bond-distances (especially for the $SiO_4$ tetrahedra), anomalous behavior of many of the atomic displacement parameters, and general problems with the stability of the refinements. Direct methods provided the locations of the Ba, Fe, Si and most O atoms in the sheets. Subsequent difference-Fourier maps revealed the locations of all remaining non-hydrogen atoms. The $PO_4$ and $CO_3$ groups in the

TABLE 1. POWDER-DIFFRACTION DATA FOR DEVITOITE

| $I_{obs}$ | $d_{obs}$ | $d_{calc}$ | $I_{calc}$ | $h$ | $k$ | $l$ | $I_{obs}$ | $d_{obs}$ | $d_{calc}$ | $I_{calc}$ | $h$ | $k$ | $l$ | $I_{obs}$ | $d_{obs}$ | $d_{calc}$ | $I_{calc}$ | $h$ | $k$ | $l$ |
|---|---|---|---|---|---|---|---|---|---|---|---|---|---|---|---|---|---|---|---|---|
| 9 | 11.43 | 11.3686 | 6 | 0 | 1 | 0 | 42 | 2.275 | 2.2821 | 11 | $\bar{1}$ | $\bar{4}$ | 1* | 27 | 1.6420 | 1.6428 | 8 | 3 | $\bar{3}$ | 2* |
| 17 | 8.77 | 8.7509 | 26 | 0 | 1 | 1 | | | 2.2730 | 13 | 0 | $\bar{2}$ | 6* | | | 1.6399 | 8 | $\bar{3}$ | 0 | 4* |
| 20 | 7.32 | 7.2794 | 24 | 0 | 0 | 2 | | | 2.2638 | 6 | 0 | $\bar{5}$ | 1 | 33 | 1.6241 | 1.6241 | 11 | 0 | 7 | 0* |
| 7 | 5.24 | 5.2076 | 8 | 0 | 2 | 1 | 35 | 2.256 | 2.2579 | 12 | 1 | $\bar{5}$ | 1 | | | 1.6230 | 12 | 0 | $\bar{7}$ | 1* |
| 53 | 4.85 | 4.8529 | 61 | 0 | 0 | 3* | | | 2.2551 | 8 | 0 | 3 | 5 | 28 | 1.5852 | 1.5841 | 12 | 1 | 3 | 7* |
| 31 | 4.33 | 4.3378 | 14 | 1 | 1 | 0 | | | 2.2341 | 9 | $\bar{1}$ | $\bar{4}$ | 2 | | | 1.5686 | 5 | 0 | 7 | 2 |
| 32 | 4.25 | 4.2636 | 30 | $\bar{1}$ | 2 | 1 | 58 | 2.225 | 2.2306 | 15 | $\bar{1}$ | 4 | 4 | | | 1.5644 | 8 | $\bar{3}$ | 5 | 1 |
| 57 | 4.02 | 4.0209 | 78 | 1 | 1 | 1* | | | 2.2219 | 39 | 2 | $\bar{1}$ | 3* | | | 1.5635 | 8 | $\bar{3}$ | $\bar{2}$ | 1 |
| 62 | 3.859 | 3.8638 | 78 | $\bar{1}$ | 2 | 2* | 32 | 2.193 | 2.1925 | 4 | 0 | 2 | 6 | | | 1.5631 | 6 | $\bar{2}$ | $\bar{4}$ | 5 |
| 38 | 3.786 | 3.7853 | 24 | 0 | $\bar{2}$ | 3 | | | 2.1924 | 5 | 2 | $\bar{2}$ | 3 | 73 | 1.5597 | 1.5618 | 5 | 3 | 0 | 3 |
| 73 | 3.629 | 3.6345 | 77 | 1 | $\bar{2}$ | 2* | | | 2.1809 | 5 | $\bar{2}$ | 4 | 1 | | | 1.5607 | 3 | $\bar{2}$ | 4 | 7 |
| | | 3.6235 | 40 | 0 | 3 | 1 | 36 | 2.172 | 2.1787 | 6 | 1 | $\bar{5}$ | 2 | | | 1.5598 | 9 | $\bar{3}$ | 5 | 0 |
| 70 | 3.457 | 3.4579 | 100 | $\bar{1}$ | $\bar{1}$ | 3* | | | 2.1690 | 6 | 2 | 0 | 3 | | | 1.5595 | 5 | $\bar{3}$ | 3 | 5 |
| 50 | 3.290 | 3.2946 | 73 | 0 | 3 | 2* | | | 2.1689 | 10 | 2 | 2 | 0 | | | 1.5594 | 4 | $\bar{1}$ | $\bar{6}$ | 4 |
| 49 | 3.143 | 3.1393 | 70 | 1 | $\bar{2}$ | 3* | | | 2.1318 | 19 | $\bar{2}$ | 4 | 2 | | | 1.5582 | 10 | $\bar{3}$ | $\bar{2}$ | 2 |
| 27 | 3.054 | 3.0619 | 14 | 0 | $\bar{3}$ | 3* | 49 | 2.120 | 2.1180 | 15 | $\bar{1}$ | $\bar{3}$ | 5 | 17 | 1.5410 | 1.5414 | 7 | 2 | $\bar{6}$ | 4 |
| | | 3.0489 | 21 | 1 | 1 | 3* | | | 2.1150 | 7 | 1 | 4 | 2 | | | 1.5375 | 4 | 1 | 2 | 8 |
| 29 | 2.976 | 2.9792 | 35 | $\bar{1}$ | $\bar{1}$ | 4* | | | 2.0978 | 12 | 1 | 3 | 4 | 11 | 1.5112 | 1.5091 | 10 | 1 | $\bar{4}$ | 8* |
| | | 2.9749 | 12 | $\bar{1}$ | $\bar{2}$ | 3 | 66 | 2.089 | 2.0911 | 31 | $\bar{2}$ | 1 | 5* | 4 | 1.4875 | 1.4874 | 3 | $\bar{2}$ | $\bar{4}$ | 6 |
| 100 | 2.911 | 2.9118 | 88 | 0 | 0 | 5* | | | 2.0802 | 9 | $\bar{2}$ | $\bar{2}$ | 3 | | | 1.4552 | 2 | $\bar{3}$ | 6 | 0 |
| 27 | 2.847 | 2.8552 | 14 | 0 | $\bar{1}$ | 5 | 30 | 1.9886 | 1.9912 | 15 | 1 | $\bar{4}$ | 5* | 13 | 1.4539 | 1.4551 | 1 | 1 | 7 | 0 |
| | | 2.8421 | 12 | 0 | 4 | 0 | | | 1.9883 | 12 | 1 | 4 | 3* | | | 1.4533 | 2 | 0 | $\bar{1}$ | 10 |
| 13 | 2.818 | 2.8161 | 10 | 0 | $\bar{4}$ | 1 | 9 | 1.9355 | 1.9423 | 3 | $\bar{1}$ | 5 | 4 | | | 1.4508 | 1 | $\bar{1}$ | 8 | 1 |
| | | 2.8119 | 7 | 1 | 0 | 4 | | | 1.9316 | 4 | 1 | $\bar{5}$ | 4 | 5 | 1.4350 | 1.4381 | 2 | 3 | $\bar{6}$ | 1 |
| 27 | 2.737 | 2.7406 | 36 | $\bar{1}$ | 4 | 1* | | | 1.8948 | 6 | 0 | 6 | 0 | | | 1.4365 | 1 | 1 | 7 | 1 |
| | | 2.6779 | 71 | $\bar{1}$ | $\bar{3}$ | 2 | 7 | 1.8913 | 1.8910 | 4 | 0 | $\bar{6}$ | 1 | 7 | 1.4209 | 1.4218 | 2 | 2 | 5 | 3 |
| 100 | 2.665 | 2.6713 | 28 | $\bar{2}$ | 1 | 1 | | | 1.8838 | 5 | 1 | 5 | 1 | 7 | 1.4209 | 1.4208 | 2 | 2 | $\bar{2}$ | 8 |
| | | 2.6575 | 76 | $\bar{2}$ | 1 | 0 | 5 | 1.8606 | 1.8648 | 4 | $\bar{1}$ | 6 | 2 | | | 1.3892 | 5 | 0 | 7 | 5 |
| 30 | 2.610 | 2.6298 | 30 | 1 | 1 | 4 | | | 1.8557 | 6 | 2 | $\bar{1}$ | 5 | 28 | 1.3821 | 1.3816 | 5 | 2 | 6 | 0* |
| | | 2.6142 | 23 | $\bar{1}$ | 4 | 2 | 6 | 1.8400 | 1.8462 | 5 | $\bar{1}$ | 4 | 6 | | | 1.3811 | 6 | 2 | $\bar{8}$ | 1* |
| 14 | 2.577 | 2.5802 | 15 | 1 | $\bar{4}$ | 2 | | | 1.8371 | 6 | 0 | $\bar{5}$ | 5 | 14 | 1.3633 | 1.3503 | 3 | 0 | $\bar{5}$ | 9 |
| 12 | 2.555 | 2.5609 | 13 | 2 | $\bar{1}$ | 1 | 11 | 1.7521 | 1.7521 | 18 | $\bar{1}$ | $\bar{3}$ | 7* | 18 | 1.3452 | 1.3437 | 4 | $\bar{2}$ | 0 | 10 |
| 14 | 2.502 | 2.5038 | 17 | $\bar{1}$ | 2 | 5* | 10 | 1.7230 | 1.7226 | 4 | 3 | 0 | 0 | | | 1.3321 | 4 | 2 | 6 | 2 |
| 9 | 2.425 | 2.4330 | 13 | $\bar{1}$ | 4 | 3 | | | 1.7222 | 5 | $\bar{3}$ | 3 | 2 | 33 | 1.3319 | 1.3308 | 5 | 3 | $\bar{5}$ | 5 |
| 10 | 2.406 | 2.4089 | 6 | 1 | 0 | 5 | 31 | 1.6901 | 1.6940 | 14 | 2 | $\bar{1}$ | 6* | | | 1.3304 | 3 | $\bar{2}$ | 2 | 10 |
| | | 2.4056 | 7 | 2 | $\bar{1}$ | 2 | | | 1.6915 | 5 | $\bar{1}$ | $\bar{2}$ | 8 | | | | | | | |
| | | | | | | | 25 | 1.6802 | 1.6858 | 5 | 3 | 0 | 1 | | | | | | | |
| | | | | | | | | | 1.6845 | 5 | $\bar{3}$ | 3 | 3 | | | | | | | |

* Used for cell refinement. Values of $d$ are expressed in Å.
Refined cell: $a$ 5.3533(3), $b$ 11.6953(5), $c$ 14.6816(8) Å, α 91.197(5), β 96.844(5), γ 103.277(5)°, $V$ 887.14(6) Å$^3$.

interlayer region exhibit somewhat anomalous features. The P–O distance for O19 had to be constrained to 1.50 Å in order for the position of this atom to refine properly. The P site refined to 75% occupancy, in reasonable agreement with results of the electron-microprobe analyses. The O atoms of the carbonate group, O20, O21 and O22, form two disordered half-occupied sets of three atoms surrounding the C site. Note that in the final refinement the occupancies of these O sites were held constant at 0.5. This resulted in a very low $U_{eq}$ of 0.005 for O21; however, if allowed to vary, the occupancy of this site refines to 0.54(13) and the $U_{eq}$, to 0.01(3). All other cation and anion sites refined best at full occupancy. Atoms OH4 and OH5 are considered to be OH based upon bond-valence summations (see below, Table 5).

With all non-hydrogen atoms located and refined anisotropically, the refinement converged to $R_1 = 9.56\%$ and $wR_2 = 24.67\%$ for 1379 reflections with $F_o > 4\sigma F$. The high $R$ values are attributed to the relatively poor quality and small size of the crystal.

The details of the data collection and the final refinement of the structure are provided in Table 2. The final atomic coordinates and displacement parameters are in Table 3. Selected interatomic distances are listed in Table 4, and bond valences, in Table 5. Tables of observed and calculated structure-factors are available from the Depository of Unpublished Data on the MAC website [document Devitoite CM48_29].

TABLE 2. DEVITOITE: DATA COLLECTION AND STRUCTURE-REFINEMENT DETAILS

| | |
|---|---|
| Diffractometer | Rigaku R-Axis Spider |
| X-ray radiation / power | MoKα (λ = 0.71075 Å) / 50 kV, 40 mA |
| Temperature | 298(2) K |
| Ideal formula | $[Ba_6(PO_4)_2(CO_3)]$ $[Fe^{2+}{}_7(OH)_4Fe^{3+}{}_2O_2(SiO_3)_8]$ |
| Space group | $P\bar{1}$ |
| Unit-cell dimensions | $a$ = 5.3437(7) Å α = 91.337(4)° |
| | $b$ = 11.6726(15) Å β = 96.757(4)° |
| | $c$ = 14.680(2) Å γ = 103.233(4)° |
| Z | 1 |
| Volume | 884.0(2) Å$^3$ |
| Density | 4.293 g/cm$^3$ (for formula above) |
| Absorption coefficient | 10.629 mm$^{-1}$ |
| $F$(000) | 1046 |
| Crystal size | 130 × 23 × 1 µm |
| θ range | 3.25 to 20.82° |
| Index ranges | $-5 \le h \le 5$, $-11 \le k \le 11$, $-14 \le l \le 14$ |
| Reflections collected / unique | 15822 / 1846 [$R_{int}$ = 0.194] |
| Reflections with $F_o > 4\sigma F$ | 1370 |
| Completeness to θ=27.46° | 99.6% |
| Refinement method | Full-matrix least-squares on $F^2$ |
| Parameters refined | 321 |
| GoF | 1.097 |
| Final $R$ indices [$F_o > 4\sigma F$] | $R_1$ = 0.0956, $wR_2$ = 0.2295 |
| $R$ indices (all data) | $R_1$ = 0.1254, $wR_2$ = 0.2467 |
| Largest diff. peak / hole | +2.59 / –1.50 $e$/Å$^3$ |

$R_{int} = \Sigma|F_o^2 - F_o^2(\text{mean})|/\Sigma[F_o^2]$. GoF = $S = \{\Sigma[w(F_o^2 - F_c^2)^2]/(n-p)\}^{1/2}$. $R_1 = \Sigma||F_o| - |F_c||/\Sigma|F_o|$. $wR_2 = \{\Sigma[w(F_o^2 - F_c^2)^2]/\Sigma[w(F_o^2)^2]\}^{1/2}$. $w = 1/[\sigma^2(F_o^2) + (aP)^2 + bP]$, where $a$ is 0.1196, $b$ is 76.7149, and $P$ is $[2F_c^2 + \text{Max}(F_o^2,0)]/3$.

## Atomic Arrangement

The most important structural unit in devitoite is a *HOH* composite sheet consisting of a layer of close-packed $Fe^{2+}O_6$ octahedra (*O*) sandwiched between heterophyllosilicate layers (*H*) (Ferraris *et al.* 1996, 2008, Ferraris 2008). The heterophyllosilicate layers are made up of open-branched *zweier* single $[Si_4O_{12}]^{8-}$ chains cross-linked by corner-sharing with $FeO_5$ tetragonal pyramids. This *HOH* sheet is essentially identical to that in astrophyllite-group minerals (Piilonen *et al.* 2003a, 2003b), except that in those, the $[Si_4O_{12}]^{8-}$ chains are usually cross-linked by $TiO_6$ octahedra. The interlayer region in the structure of devitoite contains Ba atoms, $PO_4$ tetrahedra and $CO_3$ triangles. The configuration of the Ba and $PO_4$ in the interlayer region is very similar to that in the structure of the heterophyllosilicate yoshimuraite (McDonald *et al.* 2000).

In Figure 5, we compare the structure of devitoite viewed down $a$ with similar projections of the structures of astrophyllite from Seal Lake, Labrador (LAB) (Piilonen *et al.* 2003b) and yoshimuraite. In Figure 6, we compare these structures viewed perpendicular to the sheets showing the heterophyllosilicate linkages and the placement of the large interlayer cations relative to the sheets. [Note that the cell provided in McDonald *et al.* (2000) is incorrect. The correct cell is $a$ 5.386(1), $b$ 6.999(1), $c$ 14.748(3) Å, α 95.50(2), β 93.62(2), γ 89.98(1)° (with α and γ interchanged). Also, in that paper, the $x$ coordinate of O2 should be 0.4576(9) rather than 0.9527(9). Furthermore, an incomplete cell transformation led to the mislabeling of the horizontal axis as $a$, rather than $b$ (or $b\sin\gamma$), in Figure 3 of that paper (A.M. McDonald, pers. commun.).

As in the astrophyllite-group structures, the central layer of octahedra in devitoite consists of four crystallographically distinct octahedra, Fe1, Fe2, Fe3 and Fe4, in a 2:2:2:1 ratio, respectively, and the arrangement of these octahedra within the layer is the same as in the astrophyllite-group minerals. Because of the mismatch in the size of the ideal *O* and *H* layers, a variety of distortions are required for these layers to fit together laterally in the astrophyllite sheets. These include a general flattening of the octahedra in the *H* layer, tilting of the tetrahedra in the *H* layer out of the (001) plane, and elongation of these tetrahedra along [001]. The average flattening angle (Ψ) of the octahedra in devitoite is 58.99° compared with those reported by Piilonen *et al.* (2003b) for astrophyllite-group minerals, from 58.59 to 59.41°. The most obvious general expression of these distortions, in both the astrophyllite and devitoite structures, is the wavy appearance of the sheets if viewed on edge along [100] (Fig. 5).

The size and distortions of the octahedra in astrophyllite-group minerals are significant because of the control they exert over cation ordering. Piilonen *et al.* (2003b) reported a significant and consistent variation

TABLE 3. COORDINATES AND DISPLACEMENT PARAMETERS OF ATOMS (Å$^2$) IN DEVITOITE

| | *x* | *y* | *z* | $U_{eq}$ | $U_{11}$ | $U_{22}$ | $U_{33}$ | $U_{23}$ | $U_{13}$ | $U_{12}$ |
|---|---|---|---|---|---|---|---|---|---|---|
| Ba1 | 0.5189(6) | 0.9434(2) | 0.6446(2) | 0.044(1) | 0.054(2) | 0.033(2) | 0.042(2) | 0.003(1) | 0.005(1) | 0.006(1) |
| Ba2 | 0.1665(5) | 0.2687(2) | 0.5972(2) | 0.035(1) | 0.027(2) | 0.040(2) | 0.040(2) | 0.003(1) | 0.005(1) | 0.008(1) |
| Ba3 | 0.8216(6) | 0.5529(2) | 0.6413(2) | 0.046(1) | 0.055(2) | 0.025(2) | 0.057(2) | 0.009(1) | 0.007(2) | 0.003(1) |
| Fe1 | 0.1312(11) | 0.2840(5) | 0.9829(4) | 0.029(2) | 0.025(3) | 0.021(3) | 0.040(4) | 0.007(3) | 0.006(3) | 0.005(3) |
| Fe2 | 0.7104(10) | 0.4271(5) | 0.9921(4) | 0.029(2) | 0.019(3) | 0.025(3) | 0.045(4) | 0.006(3) | 0.010(3) | 0.007(3) |
| Fe3 | 0.5655(11) | 0.1425(5) | 0.9868(4) | 0.031(2) | 0.025(3) | 0.027(3) | 0.039(4) | 0.003(3) | 0.006(3) | 0.003(3) |
| Fe4 | 0.0000 | 0.0000 | 0.0000 | 0.033(2) | 0.031(5) | 0.025(5) | 0.043(6) | 0.002(4) | 0.003(4) | 0.008(4) |
| Fe5 | 0.7271(11) | 0.2704(5) | 0.7875(4) | 0.030(2) | 0.026(3) | 0.021(3) | 0.040(4) | -0.003(3) | 0.005(3) | 0.000(3) |
| Si1 | 0.148(2) | 0.1049(8) | 0.7981(8) | 0.022(3) | 0.027(6) | 0.005(6) | 0.033(7) | 0.005(5) | 0.001(5) | 0.003(5) |
| Si2 | 0.031(2) | 0.8378(9) | 0.8225(8) | 0.028(3) | 0.023(6) | 0.013(6) | 0.046(8) | -0.004(5) | 0.007(5) | 0.000(5) |
| Si3 | 0.469(2) | 0.7085(9) | 0.8264(8) | 0.022(3) | 0.019(6) | 0.013(6) | 0.033(7) | 0.004(5) | 0.006(5) | 0.001(5) |
| Si4 | 0.319(2) | 0.4395(9) | 0.8060(8) | 0.024(3) | 0.015(6) | 0.023(7) | 0.034(7) | 0.009(5) | 0.008(5) | 0.002(5) |
| O1 | 0.200(5) | 0.132(2) | 0.910(2) | 0.034(7) | 0.04(2) | 0.01(1) | 0.06(2) | 0.02(1) | 0.00(1) | 0.01(1) |
| O2 | 0.775(4) | 0.278(2) | 0.913(2) | 0.027(7) | 0.00(1) | 0.01(1) | 0.06(2) | 0.00(1) | 0.00(1) | -0.01(1) |
| O3 | 0.068(4) | 0.850(2) | 0.932(2) | 0.016(6) | 0.01(1) | 0.01(1) | 0.02(2) | -0.01(1) | 0.00(1) | -0.01(1) |
| OH4 | 0.363(5) | 0.015(2) | 0.072(2) | 0.040(7) | 0.02(2) | 0.04(2) | 0.06(2) | -0.00(2) | 0.01(1) | 0.01(1) |
| OH5 | 0.074(5) | 0.426(2) | 0.070(2) | 0.030(7) | 0.03(2) | 0.02(2) | 0.04(2) | -0.01(1) | 0.02(1) | -0.01(1) |
| O6 | 0.492(5) | 0.288(2) | 0.062(2) | 0.026(7) | 0.02(2) | 0.01(1) | 0.05(2) | 0.01(1) | 0.01(1) | -0.00(1) |
| O7 | 0.349(4) | 0.432(2) | 0.917(2) | 0.036(7) | 0.00(1) | 0.06(2) | 0.05(2) | -0.01(2) | 0.01(1) | 0.00(1) |
| O8 | 0.738(5) | 0.766(3) | 0.785(2) | 0.061(11) | 0.02(2) | 0.11(3) | 0.03(2) | -0.02(2) | 0.01(1) | -0.03(2) |
| O9 | 0.025(5) | 0.387(3) | 0.755(2) | 0.057(10) | 0.00(1) | 0.12(3) | 0.03(2) | 0.02(2) | -0.00(1) | -0.01(2) |
| O10 | 0.238(6) | 0.774(3) | 0.786(2) | 0.058(10) | 0.08(2) | 0.10(3) | 0.02(2) | 0.01(2) | 0.01(2) | 0.08(2) |
| O11 | 0.911(6) | 0.148(4) | 0.751(2) | 0.070(11) | 0.05(2) | 0.14(4) | 0.03(2) | -0.01(2) | -0.01(2) | 0.06(2) |
| O12 | 0.515(6) | 0.385(3) | 0.760(2) | 0.047(9) | 0.05(2) | 0.06(2) | 0.05(2) | -0.01(2) | 0.02(2) | 0.05(2) |
| O13 | 0.067(7) | 0.959(2) | 0.775(2) | 0.061(10) | 0.10(3) | 0.00(2) | 0.08(3) | 0.00(2) | 0.02(2) | 0.00(2) |
| O14 | 0.381(7) | 0.576(4) | 0.783(2) | 0.084(13) | 0.08(3) | 0.12(4) | 0.04(2) | -0.02(2) | 0.01(2) | -0.01(2) |
| O15 | 0.401(6) | 0.148(3) | 0.753(2) | 0.057(10) | 0.05(2) | 0.06(2) | 0.05(2) | -0.04(2) | 0.03(2) | -0.03(2) |
| P | 0.342(3) | 0.661(1) | 0.532(1) | 0.029(4) | 0.04(1) | 0.01(1) | 0.04(1) | -0.00(1) | 0.01(1) | -0.00(1) |
| O16 | 0.171(5) | 0.732(3) | 0.569(2) | 0.044(8) | 0.04(2) | 0.05(2) | 0.05(2) | 0.01(2) | 0.01(2) | 0.01(2) |
| O17 | 0.680(6) | 0.331(3) | 0.572(2) | 0.058(9) | 0.06(2) | 0.07(2) | 0.04(2) | 0.02(2) | 0.00(2) | 0.02(2) |
| O18 | 0.606(5) | 0.733(3) | 0.569(2) | 0.041(8) | 0.02(2) | 0.06(2) | 0.04(2) | 0.00(2) | 0.00(1) | -0.01(1) |
| O19 | 0.286(5) | 0.534(2) | 0.558(2) | 0.072(12) | 0.02(2) | 0.10(3) | 0.10(3) | -0.04(2) | 0.01(2) | 0.02(2) |
| C | 0.0000 | 0.0000 | 0.5000 | 0.06(2) | 0.03(6) | 0.09(6) | 0.05(7) | 0.04(5) | -0.01(5) | 0.02(5) |
| O20 | 0.232(12) | 0.043(4) | 0.541(4) | 0.034(17) | 0.03(4) | 0.03(3) | 0.04(4) | -0.05(3) | -0.05(4) | 0.04(3) |
| O21 | 0.040(9) | 0.034(4) | 0.586(3) | 0.005(10) | 0.00(3) | 0.02(3) | 0.00(3) | -0.02(2) | -0.01(2) | 0.03(2) |
| O22 | 0.829(15) | 0.037(7) | 0.535(5) | 0.07(3) | 0.05(5) | 0.11(7) | 0.09(6) | 0.02(5) | 0.05(5) | 0.09(5) |

All atoms refined at full occupancy except P, which refined to 0.74(5), and O20, O21 and O22, which were assigned an occupancy of 0.5.

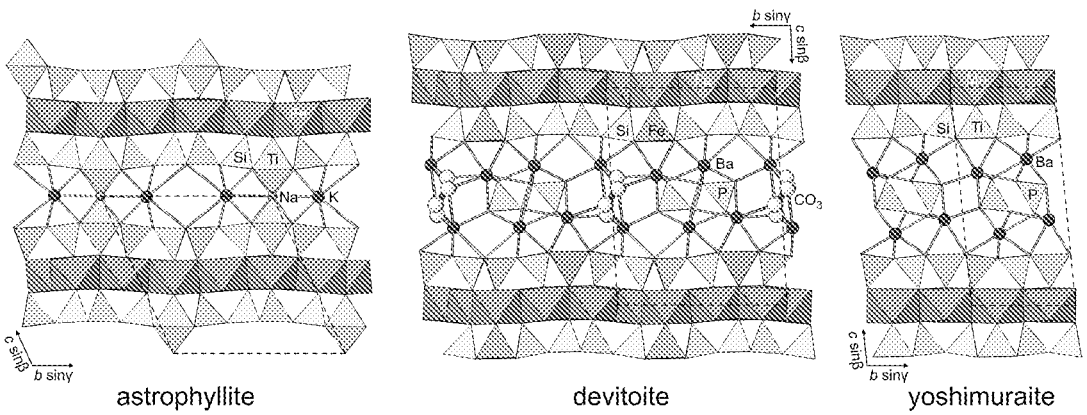


FIG. 5. Comparison of the structures of astrophyllite (LAB of Piilonen *et al.* 2003b), devitoite and yoshimuraite (McDonald *et al.* 2000), viewed parallel to the sheets.

TABLE 4. SELECTED BOND–DISTANCES (Å) AND OCTAHEDRON FLATTENING ANGLES (Ψ IN °) IN DEVITOITE

| | | | | | |
|---|---|---|---|---|---|
| Ba1 – O20 (×½) | 2.53(5) | Fe1 – O2 | 2.04(2) | Si1 – O11 | 1.56(3) |
| Ba1 – O22 (×½) | 2.54(7) | Fe1 – O6 | 2.12(2) | Si1 – O15 | 1.56(3) |
| Ba1 – O18 | 2.83(3) | Fe1 – OH5 | 2.17(2) | Si1 – O1 | 1.65(3) |
| Ba1 – O16 | 2.84(3) | Fe1 – O7 | 2.17(3) | Si1 – O13 | 1.67(3) |
| Ba1 – O21 (×½) | 2.98(5) | Fe1 – O1 | 2.17(3) | <Si1 – O> | 1.61 |
| Ba1 – O21 (×½) | 3.03(5) | Fe1 – O3 | 2.18(2) | | |
| Ba1 – O11 | 3.05(4) | <Fe1 – O> | 2.14 | Si2 – O13 | 1.57(3) |
| Ba1 – O15 | 3.07(3) | Ψ | 58.89 | Si2 – O3 | 1.60(3) |
| Ba1 – O22 (×½) | 3.09(8) | | | Si2 – O10 | 1.60(3) |
| Ba1 – O20 (×½) | 3.16(7) | Fe2 – O7 | 2.12(2) | Si2 – O8 | 1.62(3) |
| Ba1 – O10 | 3.17(3) | Fe2 – OH5 | 2.12(2) | <Si2 – O> | 1.60 |
| Ba1 – O13 | 3.27(4) | Fe2 – O6 | 2.13(2) | | |
| Ba1 – O8 | 3.27(4) | Fe2 – OH5 | 2.14(3) | Si3 – O14 | 1.60(4) |
| Ba1 – O13 | 3.29(3) | Fe2 – O2 | 2.18(2) | Si3 – O6 | 1.63(3) |
| <Ba1 – O> | 3.04 | Fe2 – O7 | 2.20(2) | Si3 – O8 | 1.63(3) |
| | | <Fe2 – O> | 2.15 | Si3 – O10 | 1.65(3) |
| Ba2 – O21 (×½) | 2.66(4) | Ψ | 59.10 | <Si3 – O> | 1.63 |
| Ba2 – O17 | 2.75(3) | | | | |
| Ba2 – O17 | 2.84(3) | Fe3 – O1 | 2.11(3) | Si4 – O12 | 1.55(3) |
| Ba2 – O20 (×½) | 2.85(4) | Fe3 – O2 | 2.12(2) | Si4 – O14 | 1.61(4) |
| Ba2 – O18 | 2.85(3) | Fe3 – O6 | 2.14(2) | Si4 – O7 | 1.62(3) |
| Ba2 – O16 | 2.86(3) | Fe3 – OH4 | 2.14(3) | Si4 – O9 | 1.63(3) |
| Ba2 – O9 | 2.92(3) | Fe3 – OH4 | 2.15(3) | <Si4 – O> | 1.60 |
| Ba2 – O12 | 2.94(3) | Fe3 – O3 | 2.15(2) | | |
| Ba2 – O22 (×½) | 2.95(9) | <Fe3 – O> | 2.14 | P – O18 | 1.50(3) |
| Ba2 – O11 | 2.99(4) | Ψ | 59.25 | P – O16 | 1.50(3) |
| Ba2 – O15 | 3.01(4) | | | P – O19 | 1.52(1) |
| Ba2 – O19 | 3.09(2) | Fe4 – OH4 (×2) | 2.06(3) | P – O17 | 1.52(3) |
| <Ba2 – O> | 2.90 | Fe4 – O3 (×2) | 2.12(2) | <P – O> | 1.51 |
| | | Fe4 – O1 (×2) | 2.22(3) | | |
| Ba3 – O17 | 2.67(3) | <Fe4 – O> | 2.13 | C – O22 (½ × 2) | 1.25(6) |
| Ba3 – O16 | 2.78(3) | Ψ | 58.73 | C – O20 (½ × 2) | 1.29(5) |
| Ba3 – O18 | 2.80(3) | | | C – O21 (½ × 2) | 1.30(5) |
| Ba3 – O9 | 2.90(3) | Fe5 – O2 | 1.83(3) | <C – O> | 1.28 |
| Ba3 – O19 | 2.93(3) | Fe5 – O9 | 1.96(3) | | |
| Ba3 – O19 | 2.94(3) | Fe5 – O12 | 1.96(3) | | |
| Ba3 – O12 | 2.98(3) | Fe5 – O15 | 1.98(3) | | |
| Ba3 – O19 | 3.02(3) | Fe5 – O11 | 2.01(3) | | |
| Ba3 – O8 | 3.36(3) | <Fe5 – O> | 1.95 | | |
| Ba3 – O14 | 3.37(4) | | | | |
| Ba3 – O14 | 3.39(4) | | | | |
| Ba3 – O10 | 3.48(4) | | | | |
| <Ba3 – O> | 3.05 | | | | |

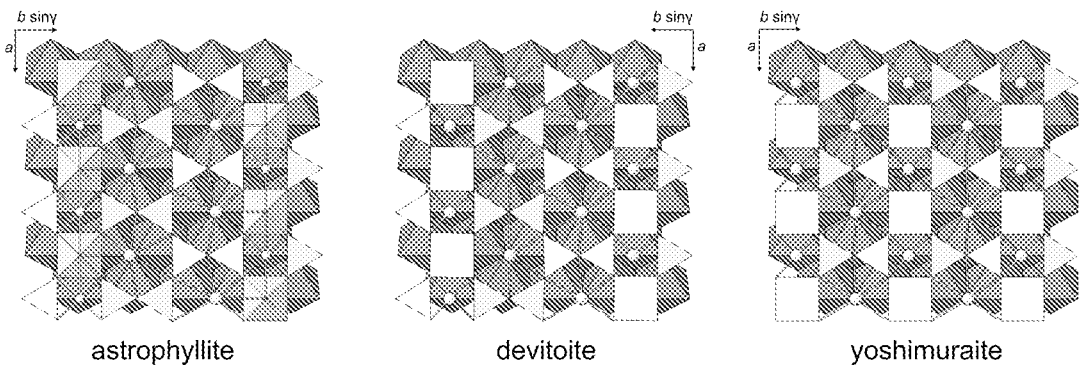


FIG. 6. Comparison of the sheet configurations in astrophyllite (LAB of Piilonen *et al.* 2003b), devitoite and yoshimuraite (McDonald *et al.* 2000), viewed perpendicular to the sheets.

in size of the octahedral sites in astrophyllite-group minerals: $M1 > M2 > M3 > M4$. In devitoite, $Fe^{2+}$ occupies all octahedral sites and, indeed, all four octahedral sites exhibit almost the same average bond-length.

The non-tetrahedral (*"hetero"*) site in the *H* layer is an octahedron in all astrophyllite-group minerals except magnesioastrophyllite (Shi et al. 1998), in which it is a tetragonal pyramid (as it is in devitoite). However, in heterophyllosilicates in general, the tetragonal pyramid is relatively commonly the non-tetrahedral component of the *H* layer, and is almost always occupied by $Ti^{4+}$ (Sokolova 2006). In fact, $Fe^{3+}$ has previously been

TABLE 5. BOND-VALENCE SUMMATIONS FOR DEVITOITE

| | Ba1 | Ba2 | Ba3 | Fe1 | Fe2 | Fe3 | Fe4 | Fe5 | Si1 | Si2 | Si3 | Si4 | P | C | $\Sigma_a v$ |
|---|---|---|---|---|---|---|---|---|---|---|---|---|---|---|---|
| O1 | | | | 0.31 | | 0.36 | 0.27 ×2↓ | | 0.93 | | | | | | 1.87 |
| O2 | | | | 0.44 | 0.30 | 0.35 | | 0.83 | | | | | | | 1.92 |
| O3 | | | | 0.30 | | 0.33 | 0.35 ×2↓ | | | 1.07 | | | | | 2.05 |
| OH4 | | | | | | 0.33<br>0.33 | 0.41 ×2↓ | | | | | | | | 1.07 |
| OH5 | | | | 0.31 | 0.35<br>0.33 | | | | | | | | | | 0.99 |
| O6 | | | | 0.35 | 0.34 | 0.33 | | | | | 0.98 | | | | 2.00 |
| O7 | | | | 0.31 | 0.35<br>0.28 | | | | | | | 1.01 | | | 1.95 |
| O8 | 0.07 | | 0.06 | | | | | | | 1.01 | 0.98 | | | | 2.12 |
| O9 | | 0.18 | 0.19 | | | | | 0.58 | | | | 0.98 | | | 1.93 |
| O10 | 0.09 | | 0.04 | | | | | | | 1.07 | 0.93 | | | | 2.13 |
| O11 | 0.13 | 0.15 | | | | | | 0.51 | 1.19 | | | | | | 1.98 |
| O12 | | 0.17 | 0.16 | | | | | 0.58 | | | | 1.22 | | | 2.13 |
| O13 | 0.07<br>0.07 | | | | | | | | 0.88 | 1.16 | | | | | 2.18 |
| O14 | | | 0.05<br>0.05 | | | | | | | | 1.07 | 1.04 | | | 2.21 |
| O15 | 0.12 | 0.14 | | | | | | 0.55 | 1.19 | | | | | | 2.00 |
| O16 | 0.23 | 0.21 | 0.27 | | | | | | | | | | 1.32 | | 2.03 |
| O17 | | 0.29<br>0.23 | 0.36 | | | | | | | | | | 1.25 | | 2.13 |
| O18 | 0.23 | 0.22 | 0.25 | | | | | | | | | | 1.32 | | 2.03 |
| O19 | | 0.12 | 0.18<br>0.17<br>0.14 | | | | | | | | | | 1.25 | | 1.86 |
| O20 | 0.26<br>0.05 | 0.11 | | | | | | | | | | | | 0.66 ×2↓ | 1.07 |
| O21 | 0.08<br>0.07 | 0.18 | | | | | | | | | | | | 0.64 ×2↓ | 0.97 |
| O22 | 0.25<br>0.06 | 0.08 | | | | | | | | | | | | 0.73 ×2↓ | 1.13 |
| $\Sigma_c v$ | 1.78 | 2.08 | 1.92 | 2.01 | 1.95 | 2.03 | 2.06 | 3.05 | 4.19 | 4.31 | 3.96 | 4.25 | 5.14 | 4.04 | |

Bond strengths from Brese & O'Keeffe (1991); valence summations are expressed in valence units (*vu*).

found to be the dominant cation in the *hetero* site in only one other heterophyllosilicate structure, that of orthoericssonite (Matsubara 1980), and may occur in the structure of ericssonite as well. Studies currently underway on the $Fe^{2+}$ analogue of ericssonite found in association with devitoite confirm that $Fe^{3+}$ occupies the square tetragonal *hetero* site in its structure.

A characteristic of *hetero* octahedra is that the Ti is displaced from the center of the octahedron toward the O atom of the layer of octahedra (*O*) (Sokolova 2006). For five-fold tetragonal pyramidal coordinations, the displacement of the Ti toward this apical O is much more extreme, resulting in a significantly shorter bond than those to the equatorial O atoms. For example, in yoshimuraite (McDonald *et al.* 2000), the average of the four equatorial Ti–O bonds is 1.961 Å compared to 1.773 Å for the apical Ti–O bond. The bond lengths for the $Fe^{3+}O_5$ tetragonal pyramid in devitoite are somewhat longer, but the displacement of the $Fe^{3+}$ toward the apical O is almost as pronounced; the average equatorial bond-length is 1.98 Å compared to the apical bond-length of 1.83 Å. The $Fe^{3+}O_5$ tetragonal pyramid in orthoericssonite (Matsubara 1980) has very similar bond-lengths, 1.992 Å equatorial *versus* 1.834 Å apical.

The cavities formed by the polyhedron linkages (four and six-membered rings) in the *H* layers in heteropyllosilicates provide sites for the large cations of the interlayer region. The placement of Ba atoms relative to the *H* (and *O*) layers in devitoite is similar to the placement of the large cations (*e.g.*, K and Na) in astrophyllite-group minerals (Fig. 6). Although the *H* layer configurations in devitoite and yoshimuraite differ, the placements of the Ba atoms and local surroundings are quite similar (Fig. 6).

The broad $[Ba_2(PO_4)]$ interlayer unit in yoshimuraite (Fig. 5) is strikingly similar to the Ba–$PO_4$ portion of the $[Ba_6(PO_4)_2(CO_3)]$ interlayer unit in devitoite. The similarities of the interlayer regions in the two structures and the manners in which they link the *HOH* sheets together are clearly indicated by the comparable *c* cell dimensions, corresponding to the sheet separations, 14.748 Å in yoshimuraite and 14.680 Å in devitoite. In yoshimuraite, the two Ba atoms, Ba1 and Ba2, are both coordinated to 11 O atoms with average bond-lengths, 2.93 and 2.87 Å, respectively. In devitoite, the three Ba atoms, Ba1, Ba2 and Ba3 are coordinated to 10.5, 11 and 12 O atoms, with average bond-lengths 3.04, 2.90 and 3.05 Å, respectively.

Only one other heterophyllosilicate, bussenite (Zhou *et al.* 2002), contains $CO_3$ in its interlayer region. However, there is no obvious similarity between the interlayer regions in the devitoite and bussenite structures. Further, in bussenite, the $CO_3$ triangle is oriented parallel to the *HOH* sheet, whereas in devitoite, it is oriented approximately perpendicular to the *HOH* sheet.

## Acknowledgements

Fernando Cámara, Elena Sokolova, Andrew M. McDonald and Stuart J. Mills provided helpful comments on the manuscript. Portions of this study were funded by the John Jago Trelawney Endowment to the Mineral Sciences Department of the Natural History Museum of Los Angeles County (ARK) and by the White Rose Foundation (GRR). Portions of this work were completed at ChemMatCARS (Sector 15) and GeoSoilEnviroCARS (Sector 13), Advanced Photon Source (APS), Argonne National Laboratory. ChemMatCARS is principally supported by the National Science Foundation and the Department of Energy under grant number NSF/CHE–0822838. GeoSoilEnviroCARS is supported by the National Science Foundation – Earth Sciences (EAR–0622171) and Department of Energy – Geosciences (DE–FG02–94ER14466). Use of the Advanced Photon Source was supported by the U.S. Department of Energy, Office of Science, Office of Basic Energy Sciences, under Contract No. DE–AC02–06CH11357.

## References

Alfors, J.T., Stinson, M.C., Matthews, R.A. & Pabst, A. (1965): Seven new barium minerals from eastern Fresno County, California. *Am. Mineral.* **50**, 314-340.

Basciano, L.C., Groat, L.A., Roberts, A.C., Gault, R.A., Dunning, G.E. & Walstrom, R.E. (2001a): Bigcreekite, a new mineral from eastern Fresno County, California. *Can. Mineral.* **39**, 761-768.

Basciano, L.C., Groat, L.A., Roberts, A.C., Grice, J.D., Dunning, G.E., Foord, E.E., Kjarsgaard, I. & Walstrom, R.E. (2001b): Kampfite, a new barium silicate carbonate mineral species from Fresno County, California. *Can. Mineral.* **39**, 1053-1058.

Brese, N.E. & O'Keeffe, M. (1991): Bond-valence parameters for solids. *Acta Crystallogr.* **B47**, 192-197.

Bruker (2005): SADABS, SAINT, SMART and SHELXTL. Bruker AXS Inc., Madison, Wisconsin.

Downs, R.T. (2006): The RRUFF Project: an integrated study of the chemistry, crystallography, Raman and infrared spectroscopy of minerals. Program and Abstracts of the 19th General Meeting of the International Mineralogical Association in Kobe, Japan. O03-13

Dunning, G.E. & Cooper, J.F., Jr. (1999): Barium silicate minerals from Trumbull Peak, Mariposa County, California. *Mineral. Rec.* **30**, 411-417.

Ferraris, G. (2008): Modular structures – the paradigmatic case of heterophyllosilicates. *Z. Kristallogr.* **223**, 76-84.

FERRARIS, G., IVALDI, G., KHOMYAKOV, A.P., SOBOLEVA, S.V., BELLUSO, E. & PAVESE, A. (1996): Nafertisite, a layer titanosilicate member of a polysomatic series including mica. *Eur. J. Mineral.* **8**, 241-249.

FERRARIS, G., MAKOVICKY, E. & MERLINO, S. (2008): *Crystallography of Modular Materials*. Oxford University Press, Oxford, U.K.

MANDARINO, J. A. (1981): The Gladstone–Dale relationship. IV. The compatibility concept and its application. *Can. Mineral.* **19**, 441-450.

MATSUBARA, S. (1980): The crystal structure of orthoericssonite. *Mineral. J.* **10**, 107-121.

MCDONALD, A.M., GRICE, J.D. & CHAO, G.Y. (2000): The crystal structure of yoshimuraite, a layered Ba–Mn–Ti silicophosphate, with comments on five-coordinated $Ti^{4+}$. *Can. Mineral.* **38**, 649-656.

NEWBERRY, N.G., ESSENE, E.J. & PEACOR, D.R. (1981): Alforsite, a new member of the apatite group: the barium analogue of chlorapatite. *Am. Mineral.* **66**, 1050-1053.

PIILONEN, P.C., LALONDE, A.E., MCDONALD, A.M., GAULT, R.A. & LARSEN, A.O. (2003a): Insights into astrophyllite-group minerals. I. Nomenclature, composition and development of a standardized general formula. *Can. Mineral.* **41**, 1-26.

PIILONEN, P.C., MCDONALD, A.M. & LALONDE, A.E. (2003b): Insights into astrophyllite-group minerals. II. Crystal chemistry. *Can. Mineral.* **41**, 27-54.

ROBERTS, A.C., GRICE, J.D., DUNNING, G.E. & VENANCE, K.E. (2001): Fencooperite, $Ba_6Fe^{3+}{}_3Si_8O_{23}(CO_3)_2Cl_3{\bullet}H_2O$, a new mineral species from Trumbull Peak, Mariposa County California. *Can. Mineral.* **39**, 1059-1064.

ROGERS, A.F. (1932): Sanbornite, a new barium silicate mineral from Mariposa County, California. *Am. Mineral.* **17**, 161-172.

ROSSMAN, G.R. & AINES, R.G. (1991): The hydrous components in garnets: grossular–hydrogrossular. *Am. Mineral.* **76**, 1153-1164.

SHELDRICK, G.M. (2008): SHELXL–97. *Program for the Refinement of Crystal Structures*. University of Göttingen, Göttingen, Germany.

SHI, N., MA, Z., LI, G., YAMNOVA, N.A. & PUSHCHAROVSKY, D.YU. (1998): Structure refinement of monoclinic astrophyllite. *Acta Crystallogr.* **B54**, 109-114.

SOKOLOVA, E. (2006): From structure topology to chemical composition. I. Structural hierarchy and stereochemistry in titanium disilicate minerals. *Can. Mineral.* **44**, 1273-1330.

WALSTROM, R.E. & LEISING, J.F. (2005): Barium minerals of the sanbornite deposits, Fresno County, California. *Axis* **1**(8), 1-18 (http://www.mineralogicalrecord.com/pdfs/Sanbornite-final.pdf).

ZHOU, H., RASTSVETAEVA, R.K., KHOMYAKOV, A.P., MA, Z. & SHI, N. (2002): Crystal structure of new mica-like titanosilicate – bussenite, $Na_2Ba_2Fe^{2+}(TiSi_2O_7)(CO_3)O(OH)(H_2O)F$. *Crystallogr. Rep.* **47**, 43-46.

*Received November 30, 2009, revised manuscript accepted February 9, 2010.*